ChemPhotoChem

Chemistry Europe
European Chemical Societies Publishing

Accepted Article

Title: Enhancement of zinc (II) phthalocyanine photophysical properties in water by sulfonatocalix[4]arene-based micelles

Authors: Sergio Dario Ezquerra Riega, Agostina Cammarata, Julieta Marino, Leonor Patricia Roguin, Romina Julieta Glisoni, and Beatriz Lantaño

To be cited as: *ChemPhotoChem* **2023**, e202300191

Link to VoR: https://doi.org/10.1002/cptc.202300191

WILEY VCH

10.1002/cptc.202300191

ENHANCEMENT OF ZINC (II) PHTHALOCYANINE PHOTOPHYSICAL PROPERTIES IN WATER BY SULFONATOCALIX[4]ARENE-BASED MICELLES

Sergio D. Ezquerra Riega[a,b], Agostina Cammarata[c], Julieta Marino[d], Leonor P. Roguin[d], Romina J. Glisoni[c]*, Beatriz Lantaño[a,b]*

[a] Dr. S. D. Ezquerra Riega, Prof. Dr. B. Lantaño

Universidad de Buenos Aires, CONICET, Facultad de Farmacia y Bioquímica, Departamento de Ciencias Químicas, Junín 956, C1113AAD Buenos Aires, Argentina.

[b] Dr. S. D. Ezquerra Riega, Prof. Dr. B. Lantaño

Universidad de Buenos Aires, Instituto de Tecnología Farmacéutica y Biofarmacia (InTecFyB), Junín 956, C1113AAD Buenos Aires, Argentina.

[c] A. Cammarata, Dr. R. J. Glisoni

Instituto NANOBIOTEC UBA-CONICET, Departamento de Tecnología Farmacéutica, Facultad de Farmacia y Bioquímica, Universidad de Buenos Aires, CABA, Buenos Aires C1113AAD, Argentina.

[d] Dr. J. Marino, Prof. Dr. L. P. Roguin

Universidad de Buenos Aires, Consejo Nacional de Investigaciones Científicas y Técnicas, Instituto de Química y Fisicoquímica Biológicas (IQUIFIB), Facultad de Farmacia y Bioquímica, Junín 956, C1113AAD Buenos Aires, Argentina.

*Corresponding author.

E-mail addresses: beatrizl@ffyb.uba.ar (B.L.); rglisoni@ffyb.uba.ar (R.J.G)

Tel.: +54-(11)-52874304 (B.L.); +54-(11)-52874652 (R.J.G.)

10.1002/cptc.202300191

Abstract

Zinc phthalocyanines have demonstrated a wide range of applications as photosensitisers, particularly in organic synthesis, photocatalysis and photodynamic therapy. Although the introduction of ionic groups on the macrocycle periphery increases their water solubility, aggregation phenomena remain as a significant drawback for their application. In this study, amphiphilic sulfonatocalix[4]arene-based micelles were used to promote the monomerization of a cationic phthalocyanine through host–guest interactions. A comprehensive spectroscopic characterization was conducted, varying the concentration of sulfonatocalix[4]arene, and binding parameters were calculated to determine the optimal conditions for complete monomerization of the photosensitizer in water. Under these conditions, the combination of sulfonatocalix[4]arene and the photosensitizer activated its photophysical activity in aqueous media, showing significant singlet oxygen photoproduction, photocatalytic capability and photostability.

10.1002/cptc.202300191

Introduction

Zinc (II) phthalocyanines (ZnPc) are excellent second-generation photosensitizers, due to their high intersystem crossing (ISC) to the first excited triplet state, high singlet oxygen photogeneration, and adequate fluorescence emission capability, and high chemical stability.[1–4] Additionally, their photophysical and chemical properties can be tuned by the introduction of different kind of substituents at the periphery of the macrocycle.[5,6] In general, monomeric ZnPc species absorption spectrum show a strong absorption maximum band ($\varepsilon_{max} \approx 10^5$ M^{-1} cm^{-1}) in the far red around 680 nm, high triplet and singlet oxygen generation quantum yields ($\Phi_\Delta > 0.5$), long triplet lifetimes ($\tau >$ 100 μs) and high stability and reduced toxicity.[7,8] As consequence, ZnPc finds a wide range of applications in industry (colorants, catalysts, photoconductors, etc.) and medicine (bioimaging, photodynamic therapy).[9–11] However, its planar, hydrophobic and extensively conjugated core structure generates the main drawbacks for its use especially in aqueous media, insolubility and aggregation.[12–14] In order to accomplish water solubility, ionic groups such as carboxy, sulfonate, phosphono, quaternary ammonium or n-alkylpyridinium groups have been successfully introduced onto the ZnPc on the periphery of the macrocycle.[14–17] Nevertheless, aggregation phenomena remain and affect the optical properties of ZnPc diminishing their photophysical efficiency, since it is well known that only monomeric form is photoactive.[18]

Nanoscale has gained great interest in the last decades and offers good opportunities to overcome the limitations mentioned above by combining ZnPc with organic, inorganic or hybrid nanomaterials.[19,20] This can be achieved through the use of different nanocarriers such as liposomes, micelles, dendrimers, polymeric nanoparticles and nanoemulsions which can partially or completely prevent aggregation and increase the solubility of ZnPc.[21] Micelles are well-defined and thermodynamically stable self-assembled nanostructures of amphiphilic molecules which only form

above a threshold concentration known as the critical micelle concentration (CMC). In general, micelles are anisotropic spherical structures with varying distribution of water, viscosity, and polarity throughout the micelle.[22] As a result, micellar nanosystems show high versatility and can interact with drugs of different polarities.[23–26]

Calix[n]arenes are macrocyclic molecules with remarkable synthetic versatility, made of n phenolic units linked in *ortho*- position to the hydroxyl group by methylene bridges (n = 4 – 20).[27],[28] In particular, calix[n]are-based surfactant can be obtained by introducing hydrophilic groups (poly(ethylene glycol) chains, carboxy, sulfonate, phosphono or quaternary ammonium groups) at one rim and hydrophobic groups (mainly n-alkyl chains) at the opposite rim.[29–31] These surfactants exhibit high affinity and selectivity in forming host-guest complexes with neutral, cationic, or anionic drugs, depending on the functional groups introduced into the calix[n]arene framework.[32] Additionally, *p*-sulfonatocalix[4]arenes bearing n-alkyl groups at the lower rim have the ability to self-assembly into micelles characterized by low CMC and toxicity and have been extensively studied.[30,33–35]

Recently, we have demonstrated that 2,9(10),16(17),23(24)-tetrakis((1-methylpyridinium-3-methyl)selanyl)phthalocyanato zinc(II) tetraiodide (**Pc3-Q**) (Scheme 1) presents excellent singlet oxygen photogeneration capability in DMSO but its photophysical properties were highly diminished in aqueous media by aggregation phenomena.[36] Herein, we investigate its incorporation into a calix[4]arene-based micellar system in order to reduce the aggregation phenomena and to obtain an efficient photoactive, water-soluble and nano-sized supramolecular system. Moreover, we compare its monomerization capability and photophysical properties with its inclusion into other micellar systems such as sodium dodecyl sulphate (**SDS**), Pluronic® F-127 and Pluronic® L-121. In particular, *p*-sulfonatocalix[4]arene tetraoctyl ether (**SSC[4]**, Scheme 1) is chosen as surfactant due to the sulfonatocalix[n]arenes well-known and extensive-described ability to form inclusion

10.1002/cptc.202300191

complexes with pyridine and (alkyl)pyridonium groups.[37] Besides, this decision is motivated by the fact that micellar properties such as CMC, size, aggregation number and stability have been reported[30,38,39] but no applications have been described yet.

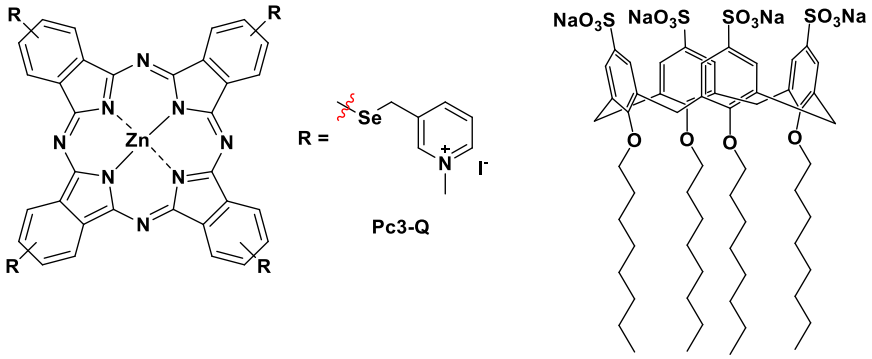

Scheme 1. Chemical structure of **Pc3-Q** and **SSC[4]**

Results and discussions

Monomerization studies

Pc3-Q is moderate soluble in aqueous medium, but it mostly self-aggregates as observed by the presence of a main absorption band at 600 nm in the absorption spectrum (Figure 1A). Besides, no fluorescence emission or singlet oxygen photoproduction was detected, showing that **Pc3-Q** is photoinactive in aqueous media (data no shown). The monomerization capability of each surfactant was evaluated over a range of concentrations from 0.1 to 10 times its CMC or until no further spectroscopic changes were observed with increasing concentration. No monomerization of **Pc3-Q** was observed in the presence of PEO-PPO micelles such as Pluronic® F-127 or L-121 triblock copolymers (Figure S1). Alternatively, the combination of **Pc3-Q** and anionic surfactant above their CMC such as **SSC[4]** (**SSC[4]@Pc3-Q**) and **SDS** (**SDS@Pc3-Q**) promoted the complete disaggregation of the photosensitizer. As it is shown in Figure 1A, modifications on **SSC[4]** concentration caused a remarkable change in the absorption spectrum of **Pc3-Q.** The rise of an absorption band at λ_{max} =

10.1002/cptc.202300191

691 nm was associated with an increase in the concentration of monomeric species until reaching complete monomerization of the photosensitizer, as confirmed by comparison with the absorption spectrum of **Pc3-Q** in DMSO. Alternately, the aggregation phenomenon also decreased as a function of SDS increased concentration, ultimately resulting in a completely disaggregated system (Figure S3).

From absorption spectra, the corresponding monomer-aggregate distribution diagram (Figure 1B) was calculated by bilinear regression, which allowed to determine the minimal ratio of **Pc3-Q** and **SSC[4]** in order to complete monomerize the photosensitizer, $r = [\mathrm{SSC[4]}]/[\mathrm{Pc3\text{-}Q}] > 161$. The same analysis was performed for **Pc3-Q** in SDS media (Figure S3), throwing a higher ratio of surfactant and **Pc3-Q** ($[\mathrm{SDS}]/[\mathrm{Pc3\text{-}Q}] > 8000$) to achieve complete monomerization.

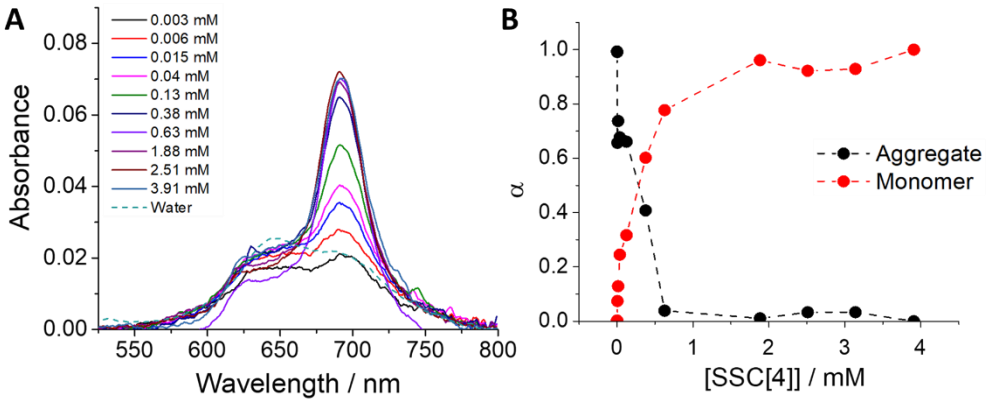

Figure 1. (A) Absorption spectra of **Pc3-Q** (6.2 µM) at different concentrations of **SSC[4]**; (B) monomer-aggregate distribution diagram calculated by bilinear regression.

Particle size, Zeta potential and cytotoxicity

Average hydrodynamic diameter (D_h), size distribution, polidispersity index (PDI) and Zeta potential (Z-pot) data of the free-drug micelles **(SSC[4])** and **SSC[4]@Pc3-Q** system are presented in Table 1, while DLS histograms and TEM images are shown in Figure 2 and Figure S4, respectively. The particle size distribution (PSD) of **SSC[4]** by intensity (%), showed two marked populations of 6 ± 2 nm and

10.1002/cptc.202300191

337 ± 144 nm, respectively, which could be assigned to micelles and micellar aggregates (Figure S4). In the same direction, DLS analysis of **SSC[4]@Pc3-Q system,** revealed the presence of two notable populations of supramolecular self-assemblies with nanometric sizes, between 7 and 212 nm (Figure 2A). The population of 7 ± 2 nm would correspond to micelles, while the population of 212 ± 84 nm, to micellar aggregates (Figure 2A). However, it could be inflicted that population of the micellar aggregates is negligible from the transformation of volume (%) obtained (Figure 2B).

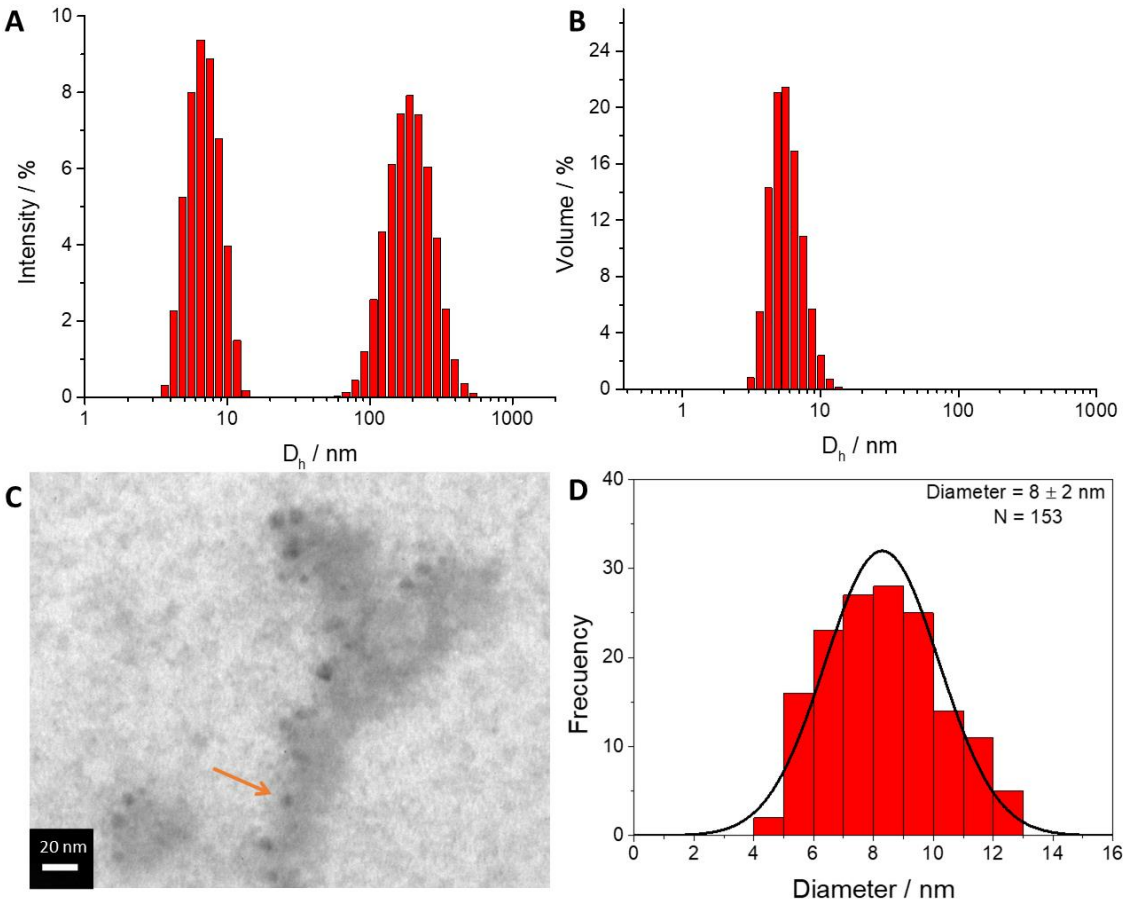

Figure 2. Particle size distribution (PSD) by DLS, expressed by: (A) Intensity (%) and (B) Volume (%). (C) TEM image of **SSC[4]@Pc3-Q** ([**Pc3-Q**] = 6.2 µM; [**SSC[4]**]=3.91 mM). Sample was stained with PTA 2% (w/v), orange arrow points out a single nanomicelle. Scale bar = 20 nm. (D) Size distribution histogram by frequency of **SSC[4]@Pc3-Q** ([**Pc3-Q**] = 6.2 µM; [**SSC[4]**]=3.91 mM) obtained from the TEM sample.

As shown in TEM images of **SSC[4]** and **SSC[4]@Pc3-Q** nanosystems (Figure 2C and Figure S4C and Figure S4E), both have spherical shapes, with an average D_h of 5 ± 2 (Figure S4D) and 8 ± 2 nm (Figura 2D), respectively, which could corresponded to a collapsed state resulting from solvent evaporation. The size of **SSC[4]** micelles agrees with the previously reported value for this calix[4]arene-based micelles.[39] However, D_h of **SSC[4]** and **SSC[4]@Pc3-Q** micelles after 3 months of tends only to the micellar aggregate populations (Figure S5), suggesting lower stability over time.

Nanosystems	D_h (±S.D.) / nm [a]	% Intensity	D_h (±S.D.) / nm [b]	PDI	ζ (±S.D.) / mV
SSC[4]	6 (2) 337 (144)	21.4 78.5	5 (1)	0.510	-25 (2)
SSC[4]@Pc3-Q	7 (2) 212 (84)	46.5 53.5	6 (2)	0.584	-19 (2)

Table 1. Hydrodynamic diameter (D_h), size distribution, polidispersity index (PDI) and Z-potential (ζ) of **SSC[4]** micelles in presence or absence of **Pc3-Q** (6.2 µM) at 25°C. [a]PSD by Intensity (%) and [b]PSD by Volume(%)

As resumed in Table 1, a less negative Z-pot value (Z-pot = -19mV, Table 1) was observed for **SSC[4]@Pc3-Q** due to the cationic nature of the guest which partially compensates the negative nature of the micellar host (Z-pot = -25mV, Table 1). Taking into account these results, we suggested that **Pc3-Q** is possibly located on the surface of micelles, through an electrostatic interaction, and **SSC[4]@Pc3-Q** remains stable in aqueous media. As well as it was described for **SSC[4]**-based micellar systems, two marked populations were observed by DLS, for **SDS** micellar system and **SDS@Pc3-Q**, where the smaller population would correspond to micelles, it was predominant (Table S2 and Figure S6). Moreover, the Z-potential values of SDS micelles became less negative in presence of **Pc3-Q,** as a result of charge compensation on the micelle surface.

In vitro cytotoxicity of **SSC[4]** and **SDS** micelles was evaluated by MTT assay on CT26 and LM3 cell lines. As shown in Figure S8, **SSC[4]** showed lower toxicity than SDS with an IC_{50} of 0.12 ± 0.02 mM and 2.5 ± 0.3 mM, respectively. However, despite showing good singlet oxygen photoproduction

capability (*vide infra*), **SSC[4]@Pc3-Q** showed no increase in the phototoxicity. Since cellular uptake of nanomaterials is dependent on their physicochemical properties, including particle size, shape and surface charge[40–43], it could be hypothesized that highly negatively charged micellar aggregates (Figure S7) are less efficiently internalized by cells, although the lack of photoactivity requires further investigation.

Binding Ability and Thermodynamic Parameters

The spectroscopic changes were analysed using the Benesi-Hildebrand binding model which has been largely employed to study micellar-drug interactions, considering the concentration of micellar aggregates negligible in solution.[44,45] As shown in Figure 3, the application of Benesi-Hildebrand equation, which the best fit was achieved by using equimolar stoichiometry, enabled to identify two different equilibria according to the range of surfactant concentration used. Moreover, it was calculated that the transition between equilibria occurs at [**SSC[4]**] = 0.07 ± 0.02 mM which is consistent with the CMC reported for **SSC[4]** ($CMC_{SSC[4]}$ = 0.09 ± 0.01 mM[30,38]). Analogously, the binding analysis between **Pc3-Q** and **SDS** by Benesi-Hildebrand model showed the presence of two equilibria with equimolar stoichiometry and a transition concentration equal to the CMC, [SDS] = 7 ± 2 mM (CMC_{SDS} = 8 mM[46] ; Figure S9).

10.1002/cptc.202300191

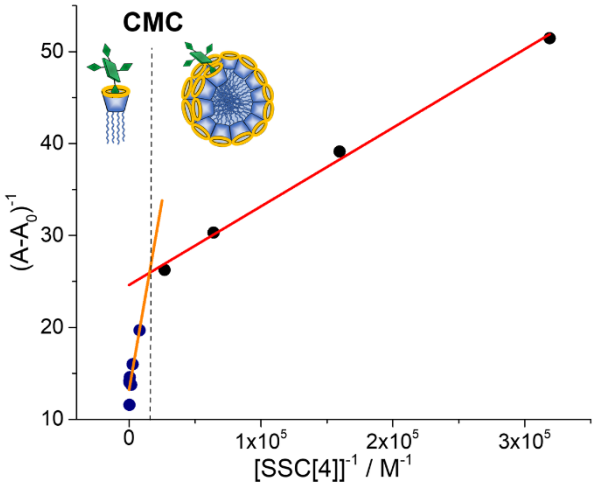

Figure 3. Benesi-Hildebrand plot for the binding interaction of **Pc3-Q** with **SSC[4]** and pictorial representation of **SSC[4]@Pc3-Q** based on experimental results.

Therefore, we were able to infer in both cases that monomerization of **Pc3-Q** at low concentration of **SSC[4]** is produced by the formation of a binding complex between the surfactant monomer and **Pc3-Q**, meanwhile the proper micelle is the complexing agent above the CMC.

Besides, thermodynamic binding constant (K_b) was obtained from the fitting for each proposed equilibrium and the corresponding Gibbs free energy (ΔG_b) was calculated using the familiar relationship, $\Delta G_b = -RT \ln K_b$ in which R and T refer to the gas constant and the absolute temperature, respectively. As shown in Table 2, complex formation above CMC is less favoured in presence of both surfactant which can be associated to repulsion forces between sulfonate groups of different monomers at micelle surface. Additionally, both **SSC[4]** as monomer and micelle show a remarkable increase binding affinity with **Pc3-Q** compared to the corresponding SDS species. These differences can be explained by the capability of sulfonatocalix[n]arene to form binding complexes with pyridine and N-methylpyridinium groups. Thus, the ΔG_b for both species of **SSC[4]** and **Pc3-Q** are in agreement with those reported for the complexation of calix[4]arene tetrasulfonate and N-methylpyridinum ions.[32,37] Therefore, we conclude that the electrostatic

interactions and complexation between the **SSC[4]** cavity and a N-methylpyridinium group in peripherical position of **Pc3-Q** are the main forces for the nanophotosystem formation and monomerization of the photosensitizer.

N-methyl pyridinium interaction with **SSC[4]** was also evidenced by NMR experiments in D_2O using a N-methyl pyridinium phthalonitrile as a simple guest model of **Pc3-Q**. As shown in Figure S10, the signals of the pyridine ring and N-methyl group are strongly shifted upfield after the addition of **SSC[4]**. The upfield variation of these signals ($\Delta\delta = \delta_{complex} - \delta_{free} < 0$) is induced by the ring current effect of the aromatic nuclei of sulfonatocalix[4]arene and shows similar values to those already reported for similar binding complexes.[37,47] Therefore, these changes agree with the formation of a stable supramolecular complex where the N-methyl pyridinium group of the guest is engulfed inside the **SSC[4]** cavity. Taking into account all these results, a probable representation for **SSC[4]@Pc3-Q** is proposed where only a pyridinium group of **Pc3-Q** is entrapped within the cavity of a **SSC[4]** monomer of the micelle (Figure 3).

Additionally, partitions parameters ($\mathrm{K_p}$ and $\Delta\mathrm{G_p}$) were calculated by pseudo phase model (Table S4). Both photoactive nanoassemblies show that the leaking of **Pc3-Q** from the nanosystem to aqueous media is highly disfavour. In particular, assemblies based on **SSC[4]** micelles are more stable against the release of **Pc3-Q**.

10.1002/cptc.202300191

Nanosystems	K_b / M^{-1}	ΔG_b / kJ mol^{-1}
SSC[4]$_{Monomer}$@Pc3-Q	(2.9 ± 0.2) 10^5	-31.2 ± 0.5
SSC[4]@Pc3-Q	(7 ± 1) 10^4	-27.8 ± 0.5
SDS$_{Monomer}$@Pc3-Q	(5.5 ± 0.3) 10^3	-21 ± 1
SDS@Pc3-Q	350 ± 40	-14.5 ± 0.3
(SC4ABu)@py$^+$CH$_3$ [37]	9 x 10^4 – 10^6	- (28 – 34)

Table 2. Binding thermodynamic parameters calculated from Benesi-Hildebrand equation. **(SC4ABu)@py$^+$CH$_3$**: N-methylpyridinium and sodium 25,26,27,28-tetrabutyl calix[4]arene tetrasulfonate binding complex.

Alternately, non-linear fitting using equation S7 showed good agreement with experimental absorption data (Figure 4A) and allowed to estimate the surfactant CMC and the binding constant for **SSC[4]@Pc3-Q**. Additionally, fluorescence emission and singlet oxygen photoproduction capability were studied as function of **SSC[4]** (Figure S11 and Figure S12). As shown in Figure 4-B, all photophysical parameters showed similar behaviour to previously observe through absorption and non-linear analysis were performed using equation S7 adequate modified. The increase of photoactivity was associated with the monomerization of **Pc3-Q** by the formation of the **SSC[4]@Pc3-Q**. CMC and K_b parameters obtained from each non-linear fit were consistent with those previously calculated by Benesi-Hildebrand equation (Table S5). Similar analysis was performed for **SDS@Pc3-Q,** showing similar dependency between the photophysical properties and the monomerization degree (Figure S13).

10.1002/cptc.202300191

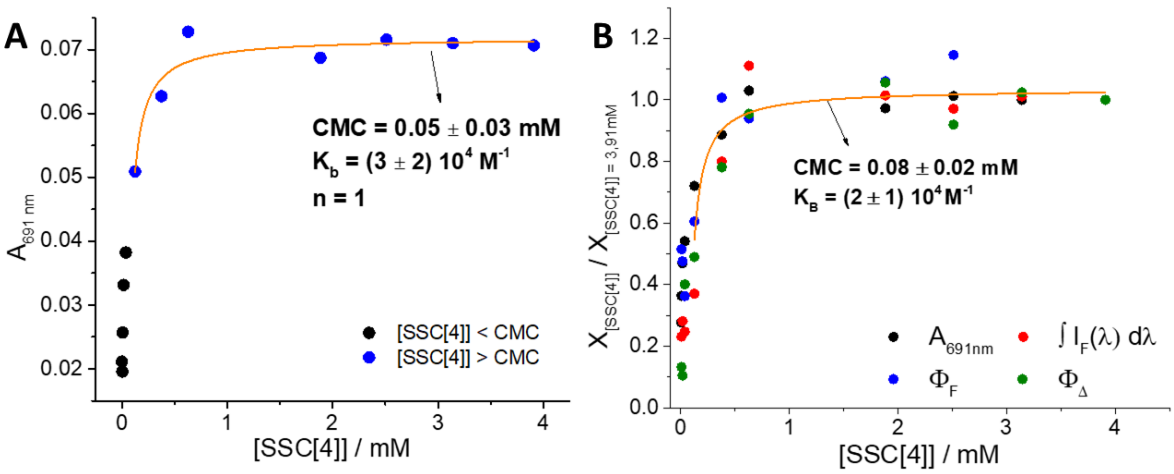

Figure 4. (A) Absorbance and (B) relative photophysical parameters of **Pc3-Q** as function of **SSC[4]** concentration. Solid line is the corresponding (average) non-linear fit.

Photophysical characterization of nanoassemblies

Relevant spectra for **SSC[4]@Pc3-Q** are shown in Figure 5 and the photophysical parameters of photoactive nanoassemblies are resumed in Table 3. All parameters were measured at least twice above of previously calculated minimal ratio (r) of reagents for complete monomerization of **Pc3-Q**. Firstly, no significant spectral change (shape and shifting) was observed when compared to the reported spectra **of Pc3-Q** in DMSO.[36] However, the absorption coefficient ($\varepsilon_{\lambda_{max}}$) of **Pc3-Q** in both micellar media was shown to be an order of magnitude lower than the value reported in DMSO. On the other hand, the agreement between the excitation and absorption spectra of **SSC[4]@Pc3-Q** within the experimental error (Soret band region was obtained by difference of micellar system and nanophotoassembly spectra) inferred that Kasha's rule is fulfilled (Figure 5).

10.1002/cptc.202300191

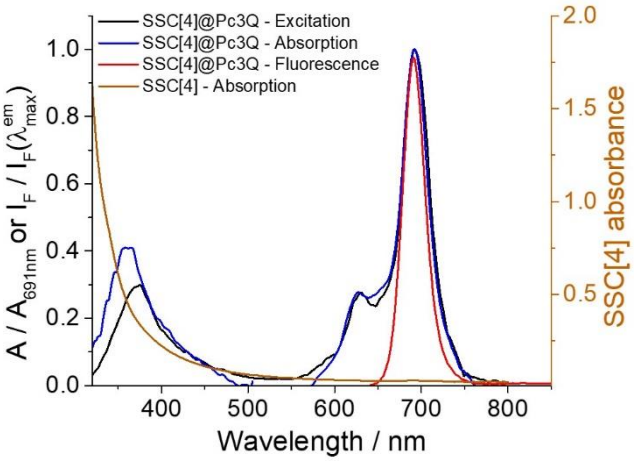

Figure 5. Normalized absorption, emission and excitation spectra of **SSC[4]@Pc3-Q**. [**SSC[4]**] = 3.91 mM

Φ_F of **SSC[4]@Pc3-Q** were found to be significantly lower than the corresponding value measured for **Pc3-Q** in DMSO and SDS micelles. The observed difference can be associated to the increase of internal conversion process as a result of the formation of the inclusion complexes.

An indirect methodology was employed to quantify singlet oxygen production, through the use of methylene blue as reference and 9,10- anthracenediyl-bis(methylene)dimalonic acid potassium salt (ABDA) which is a well-documented, water soluble and singlet oxygen specific chemical monitor.[48] Furthermore, ABDA showed no photodegradation upon irradiation in absence of photosensitizer while its concentration significantly decreased in presence of **SSC[4]@Pc3-Q** (Figure S17). As Table 3 shown, the Φ_Δ of **SSC[4]@Pc3-Q** and **SDS@Pc3-Q** were significantly lower than the value measured for **Pc3-Q** in DMSO. Taking into account that photoproduced singlet oxygen is capable of diffusing into the micelle and the distance between chemical monitor and micelle surface is influenced by electrostatic repulsion, experimentally obtained Φ_Δ values are underestimated and refer to the quenchable fraction of $^1O_2$ by ABDA. Despite showing a low quenchable Φ_Δ, this value is similar to and even higher than Φ_Δ reported for other phthalocyanines entrapped in polymeric micelles.[49]

10.1002/cptc.202300191

Photophysical properties	Pc3-Q [a,36]	Pc3-Q@SSC[4] [b]	Pc3-Q@SDS [c]
λ_{max}/ nm	690.5	691	687
$\varepsilon_{\lambda_{max}}$ / $cm^{-1}M^{-1}$	(2.49 ± 0.05) 10^5	(1.2 ± 0.1) 10^4	(1.5 ± 0.03) 10^4
λ_{max}^{exc}/ nm	691	690	688
λ_{max}^{em}/ nm	695	693	693
$\Delta\lambda$ / nm	4	3	5
Φ_F	0.13 ± 0.02	0.04 ± 0.01	0.09 ± 0.02
Φ_Δ	0.61 ± 0.03	0.34 ± 0.03	0.38 ± 0.03
k_p / min^{-1}	(1.13 ± 0.03) 10^{-4}	(9.3 ± 0.4) 10^{-5}	(3.1 ± 0.2) 10^{-4}

Table 3. Photophysical properties of **Pc3-Q** in different media. [a]DMSO; [b][**SSC[4]**]=3.91 mM; [c][SDS]=133 mM.

The photocatalytic activity of **SSC[4]@Pc3-Q** was also assayed by degrading methyl orange (**MO**), a synthetic azo dye commonly found in industrial effluents, using selective irradiation of the **SSC[4]**, **SSC[4]@Pc3-Q** and Rose Bengal (**RB**; a known water soluble singlet oxygen generator; Φ_Δ = 0.76[50]).[51] The photoinduced bleaching of **MO** was analysed by using the initial rate method. Despite of the significant singlet oxygen photoproduction capability difference, the initial photodegradation rate of **MO** in presence of **SSC[4]@Pc3-Q** was significantly higher than the rate observed by **RB** (Figure S18). The difference can be explained by the kind of interaction between the model pollutant and each photosensitizer. **MO** (pKa = 3.46[52]) and **RB** (pKa_1 = 1.89; pKa_2 = 3.93[53]) are both anionic compounds at neutral pH, and, therefore, electrostatic repulsion plays an important role as spacer between the photogenerated singlet oxygen and **MO.**[54] Instead, the higher degradation rate of **MO** in the presence **SSC[4]@Pc3-Q** can be attributed to a smaller distance between **MO** and **Pc3-Q**, leading to a higher local **MO** concentration on micelle surface due to the complexation of the azo dye and **SSC[4]**. This interaction is driven by the engulfment of N,N-dimethyl amino group within calix[4]arene cavity.[55]

Besides, negligible photodegradation of the **Pc3-Q** was observed upon irradiation of **SSC[4]@Pc3-Q** and its stability was significantly increased by 20-fold and 230-fold compared to **Pc3-Q** in DMSO and **SDS@Pc3-Q**, respectively (Table 3 and Figure S19).

Conclusion

We have demonstrated that sulfonatocalix[4]arene-based micelles, such as **SSC[4]**, represent a versatile supramolecular host for complexing and monomerizing a zinc (II) phthalocyanine properly substituted with terminal pyridinium groups, as **Pc3-Q,** in aqueous media. A clear in-depth study about **SSC[4]@Pc3-Q** micelles was obtained from the complementary analysis of DLS, TEM, NMR experiments and thermodynamic assays. The formation of **SSC[4]@Pc3-Q** switches on the photophysical activity of **Pc3-Q** in water, leading to significant singlet oxygen photoproduction. Furthermore, **SSC[4]@Pc3-Q** has shown to be highly photostable. Based on our results, **SSC[4]@Pc3-Q** result a potential candidate to be tested as photocatalyst in organic synthesis reactions in aqueous media, such as oxidation or pefluoroalkylation reactions among others.

Experimental section

Chemistry

Pc3-Q was synthetized in our lab according to the procedure previously reported.[36] The synthesis of **SSC[4]** was carried out using previously described methodologies with slightly modifications which can be observed in the Supporting Information.

Instrumentation

^{1}H NMR and ^{13}C NMR were recorded on NMR Bruker AVANCE III 600 MHz (14.1 T) Spectrometer at room temperature (25 ± 2 °C). Chemical shifts (δ) are reported relative to tetramethylsilane (TMS) as an internal standard. Spin multiplicities are indicated as s, bs, d, dd, t, and m. The coupling

constants (J) are given in Hz. Electronic absorption spectra were determined with a Jasco V-570 UV-Vis spectrophotometer. Fluorescence and excitation spectra were recorded with a Perkin-Elmer LS-55 spectrofluorometer. The hydrodynamic diameter (D_h), the polydispersity index (PDI), the zeta potential (Z-Potential), of the **SSC[4]@Pc3-Q** at 25°C were measured by Dynamic Light Scattering (DLS) using a Nano-ZS Zetasizer with Non-Invasive Back Scatter (NIBS®) technology (Malvern Ltd., Malvern, UK). As controls, **SSC[4]** and **SDS and SDS@Pc3-Q** were analyzed in the same conditions. Determinations were performed at a fixed scattering angle of 173° and fixed laser position 4.65 mm, He-Ne laser (633 nm), and a digital correlator (ZEN3600). For Z-Potential, laser Doppler micro-electrophoresis is used. The refraction indexes (IR) was 1.33 for the solvent and the refraction index of **SSC[4]** was estimated at 1.46 according reported literature[56]. Viscosities were between 0.8869 and 0.8876 cP at 25 °C. Each sample was analyzed in triplicate, and the values were counted as an average with six measurements each. Transmission electronic microscopy (TEM) images were obtained using a Zeiss EM 109T equipped with a digital camera Gatan ES1000W (Germany). Samples were stained with phosphotungstic acid 2% (w/v) (PTA) or uranyl acetate (UA).

Preparation of the photoactive nanoassemblies

PEO-PPO copolymers, **SDS** and **SSC[4]** stock dispersions were prepared by dissolving the proper amount of each surfactant in 10 mL of mili-Q quality water. The dispersions were stored at 4°C for 24 hours, then stirred for 12 hours at room temperature and finally, filtered with 0.45 µm nylon filter to remove any residual aggregates.[57,58] All range-concentration surfactant dispersions were prepared by dilution of the stock dispersion. Photoactive nanoassemblies were obtained by mixing well-defined surfactant solution and **Pc3-Q** stock solution (318 µM). The mixture was stirred by inversion for a minute and filtered with 0.45 µm nylon filter. Micellar (photo)systems were stored protected from light and at a low temperature between 0 and 4°C up to 3 months without showing macroscopic or spectroscopic changes.

Supporting Information

The authors have cited additional references within the Supporting Information.[59–71]

Acknowledgments

This work was supported by grants from the University of Buenos Aires, (Programación científica 2018–2020, UBACyT 20020170200301BA) and the Agencia Nacional de Promoción Científica y Tecnológica (PICT 2019-3331) Buenos Aires, Argentina. We would like to thank Dr. Hernán B. Rodríguez for sharing the Excel-based bilinear regression software and fruitful discussions.

Keywords: sulfonatocalix[4]arene, phthalocyanines, micelles, monomerization, singlet oxygen.

References

[1] C. M. Allen, W. M. Sharman, J. E. Van Lier, *J. Porphyr. Phthalocyanines* **2001**, *05*, 161–169.

[2] I. J. Macdonald, T. J. Dougherty, *J. Porphyr. Phthalocyanines* **2001**, *05*, 105–129.

[3] M. R. Detty, S. L. Gibson, S. J. Wagner, *J. Med. Chem.* **2004**, *47*, 3897–3915.

[4] S. Moeno, R. W. M. Krause, E. A. Ermilov, W. Kuzyniak, M. Höpfner, *Photochem. Photobiol. Sci.* **2014**, *13*, 963–970.

[5] C. A. Strassert, G. M. Bilmes, J. Awruch, L. E. Dicelio, *Photochem. Photobiol. Sci.* **2008**, *7*, 738–747.

[6] G. A. Gauna, J. Marino, M. C. García Vior, L. P. Roguin, J. Awruch, *Eur. J. Med. Chem.* **2011**, *46*, 5532–5539.

[7] L. P. Roguin, N. Chiarante, M. C. García Vior, J. Marino, *Int. J. Biochem. Cell Biol.* **2019**, *114*, 105575.

[8] D. A. Fernández, J. Awruch, L. E. Dicelio, *Photochem. Photobiol.* **1996**, *63*, 784–792.

[9] Y. Zhang, J. F. Lovell, *WIREs Nanomedicine and Nanobiotechnology* **2017**, *9*, e1420.

[10] C. G. Claessens, U. Hahn, T. Torres, *Chem. Rec.* **2008**, *8*, 75–97.

[11] D. Wöhrle, G. Schnurpfeil, S. G. Makarov, A. Kazarin, O. N. Suvorova, *Macroheterocycles* **2012**, *5*, 191–202.

[12] D. A. Fernández, J. Awruch, L. E. Dicelio, *J. Photochem. Photobiol. B Biol.* **1997**, *41*, 227–232.

[13] M. E. Rodriguez, D. A. Fernández, J. Awruch, S. E. Braslavsky, L. E. Dicelio, *J. Porphyr. Phthalocyanines* **2006**, *10*, 33–42.

[14] J. Marino, M. C. García Vior, L. E. Dicelio, L. P. Roguin, J. Awruch, *Eur. J. Med. Chem.* **2010**, *45*, 4129–4139.

[15] N. Sekkat, H. Van Den Bergh, T. Nyokong, N. Lange, *Molecules* **2012**, *17*, 98–144.

[16] N. Brasseur, R. Ouellet, C. La Madeleine, J. Van Lier, *Br. J. Cancer* **1999**, *80*, 1533–1541.

[17] E. Güzel, A. Koca, M. B. Koçak, *Supramol. Chem.* **2017**, *29*, 536–546.

[18] Y. N. Konan, R. Gurny, E. Allémann, *J. Photochem. Photobiol. B Biol.* **2002**, *66*, 89–106.

[19] S. Wang, R. Gao, F. Zhou, M. Selke, *J. Mater. Chem.* **2004**, *14*, 487–493.

[20] S. S. Lucky, K. C. Soo, Y. Zhang, *Chem. Rev.* **2015**, *115*, 1990–2042.

[21] M. C. García Vior, J. Marino, L. P. Roguin, A. Sosnik, J. Awruch, *Photochem. Photobiol.* **2013**, *89*, 492–500.

[22] G. B. Dutt, *J. Phys. Chem. B* **2003**, *107*, 10546–10551.

[23] V. P. Torchilin, *J. Control. Release* **2001**, *73*, 137–172.

[24] A. Ianiro, Á. González García, S. Wijker, J. P. Patterson, A. C. C. Esteves, R. Tuinier, *Langmuir* **2019**, *35*, 4776–4786.

[25] Z. Vinarov, V. Katev, D. Radeva, S. Tcholakova, N. D. Denkov, *Drug Dev. Ind. Pharm.* **2018**, *44*, 677–686.

[26] T. S. Banipal, H. Kaur, P. K. Banipal, *J. Therm. Anal. Calorim.* **2017**, *128*, 501–511.

[27] C. D. Gutsche, *Calixarenes Revisited*, Royal Society Of Chemistry, Cambridge, **1998**.

[28] G. M. L. Consoli, G. Granata, C. Geraci, in *Des. Dev. New Nanocarriers*, Elsevier, **2018**, pp. 89–143.

[29] Y. Cakmak, T. Nalbantoglu, T. Durgut, E. U. Akkaya, *Tetrahedron Lett.* **2014**, *55*, 538–540.

[30] N. Basílio, L. Garcia-Rio, *ChemPhysChem* **2012**, *13*, 2368–2376.

[31] M. Strobel, K. Kita-Tokarczyk, A. Taubert, C. Vebert, P. A. Heiney, M. Chami, W. Meier, *Adv. Funct. Mater.* **2006**, *16*, 252–259.

[32] Y. Liu, E.-C. Yang, Y. Chen, D.-S. Guo, F. Ding, *European J. Org. Chem.* **2005**, *2005*, 4581–4588.

[33] S. Shinkai, T. Arimura, K. Araki, H. Kawabata, H. Satoh, T. Tsubaki, O. Manabe, J. Sunamoto, *J. Chem. Soc. Perkin Trans. 1* **1989**, 2039–2045.

[34] L. Baldini, A. Casnati, F. Sansone, R. Ungaro, *Chem. Soc. Rev.* **2007**, *36*, 254–266.

[35] F. Perret, A. N. Lazar, A. W. Coleman, *Chem. Commun.* **2006**, 2425–2438.

[36] S. D. Ezquerra Riega, F. Valli, H. B. Rodríguez, J. Marino, L. P. Roguin, B. Lantaño, M. C.

García Vior, *Dye. Pigment.* **2022**, *201*, 110110.

[37] X.-Y. Hu, S. Peng, D.-S. Guo, F. Ding, Y. Liu, *Supramol. Chem.* **2015**, *27*, 336–345.

[38] N. Basiílio, L. Garcia-Rio, M. Martiín-Pastor, *Langmuir* **2012**, *28*, 2404–2414.

[39] S. Fujii, J. H. Lee, R. Takahashi, K. Sakurai, *Langmuir* **2018**, *34*, 5072–5078.

[40] S. M. A. Sadat, S. T. Jahan, A. Haddadi, *J. Biomater. Nanobiotechnol.* **2016**, *07*, 91–108.

[41] D. Zhang, L. Wei, M. Zhong, L. Xiao, H.-W. Li, J. Wang, *Chem. Sci.* **2018**, *9*, 5260–5269.

[42] Q. Huo, J. Zhu, Y. Niu, H. Shi, Y. Gong, Y. Li, H. Song, Y. Liu, *Int. J. Nanomedicine* **2017**, *12*, 8631–8647.

[43] S. Jeon, J. Clavadetscher, D.-K. Lee, S. Chankeshwara, M. Bradley, W.-S. Cho, *Nanomaterials* **2018**, *8*, 1028.

[44] N. Azum, M. A. Rub, S. Y. Alfaifi, A. M. Asiri, *Polymers (Basel).* **2021**, *13*, 1214.

[45] M. Enache, A. M. Toader, V. Neacsu, G. Ionita, M. I. Enache, *Molecules* **2017**, *22*, 1079.

[46] A. M. Khan, S. S. Shah, *J. Chem. Soc. Pakistan* **2008**, *30*, 186–191.

[47] G. Arena, A. Casnati, A. Contino, G. G. Lombardo, D. Sciotto, R. Ungaro, *Chem. - A Eur. J.* **1999**, *5*, 738–744.

[48] T. Entradas, S. Waldron, M. Volk, *J. Photochem. Photobiol. B Biol.* **2020**, *204*, 111787.

[49] M. C. García Vior, J. Marino, L. P. Roguin, A. Sosnik, J. Awruch, *Photochem. Photobiol.* **2013**, *89*, 492–500.

[50] F. Wilkinson, W. P. Helman, A. B. Ross, *J. Phys. Chem. Ref. Data* **1993**, *22*, 113–262.

[51] A. Sindelo, J. Britton, A. E. Lanterna, J. C. Scaiano, T. Nyokong, *J. Photochem. Photobiol. A Chem.* **2022**, *432*, 114127.

[52] H. Kahlert, G. Meyer, A. Albrecht, *ChemTexts* **2016**, *2*, 1–28.

[53] V. R. Batistela, D. S. Pellosi, F. D. De Souza, W. F. Da Costa, S. M. De Oliveira Santin, V. R. De Souza, W. Caetano, H. P. M. De Oliveira, I. S. Scarminio, N. Hioka, *Spectrochim. Acta - Part A Mol. Biomol. Spectrosc.* **2011**, *79*, 889–897.

[54] J. J. Romero, J. H. Hodak, H. B. Rodríguez, M. C. Gonzalez, *J. Phys. Chem. C* **2018**, *122*, 26865–26875.

[55] S. Shinkai, K. Araki, O. Manabe, *J. Chem. Soc., Chem. Commun.* **1988**, 187–189.

[56] A. V. Nabok, T. Richardson, C. McCartney, N. Cowlam, F. Davis, C. J. M. Stirling, A. K. Ray, V. Gacem, A. Gibaud, *Thin Solid Films* **1998**, *327–329*, 510–514.

[57] R. J. Glisoni, A. Sosnik, *J. Nanosci. Nanotechnol.* **2014**, *14*, 4670–4682.

[58] R. J. Glisoni, A. Sosnik, *Macromol. Biosci.* **2014**, *14*, 1639–1651.

[59] S. A. Senthan, V. Alexander, *New J. Chem.* **2016**, *40*, 10064–10070.

[60] V. S. Sharma, A. P. Shah, A. S. Sharma, *New J. Chem.* **2019**, *43*, 3556–3564.

[61] E. Nomura, A. Hosoda, M. Takagaki, H. Mori, Y. Miyake, M. Shibakami, H. Taniguchi, *Langmuir* **2010**, *26*, 10266–10270.

[62] Z. Qin, D. S. Guo, X. N. Gao, Y. Liu, *Soft Matter* **2014**, *10*, 2253–2263.

[63] A. Ogunsipe, D. Maree, T. Nyokong, *J. Mol. Struct.* **2003**, *650*, 131–140.

[64] R. W. Redmond, J. N. Gamlin, *Photochem. Photobiol.* **1999**, *70*, 391–475.

[65] C. Meenakshi, P. Jayabal, V. Ramakrishnan, *Spectrochim. Acta - Part A Mol. Biomol. Spectrosc.* **2015**, *151*, 707–711.

[66] P. S. Santiago, S. C. M. Gandini, L. M. Moreira, M. Tabak, *J. Porphyr. Phthalocyanines* **2008**, *12*, 942–952.

[67] H. Kawamura, M. Manabe, Y. Miyamoto, Y. Fujita, S. Tokunaga, *J. Phys. Chem.* **1989**, *93*, 5536–5540.

[68] R. Aroca, T. Del Caño, J. A. De Saja, *Chem. Mater.* **2003**, *15*, 38–45.

[69] E. Venuti, R. G. Della Valle, I. Bilotti, A. Brillante, M. Cavallini, A. Calò, Y. H. Geerts, *J. Phys. Chem. C* **2011**, *115*, 12150–12157.

[70] S. Hammer, T. Ferschke, G. V. Eyb, J. Pflaum, *Appl. Phys. Lett.* **2019**, *115*, 263303.

[71] Z. Fan, C. Cheng, S. Yu, K. Ye, R. Sheng, D. Xia, C. Ma, X. Wang, Y. Chang, G. Du, *Opt. Mater. (Amst).* **2009**, *31*, 889–894.

10.1002/cptc.202300191

Entry for the Table of Contents

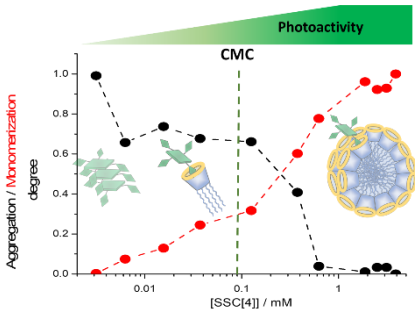

Full monomerization of a N-methylpyridinium tetrasubstituted zinc phthalocyanine in aqueous media can be achieved through its interaction with sulfonatocalix[4]arene-based micelles. The nanophotoactive systems show significant photophysical activity in aqueous media, particularly in singlet oxygen photoproduction, which is completely null in the absence of the surfactant.